Dual-Readout Calorimetry for High-Quality Energy Measurements

Progress Report

Presented by:

Dr. Gabriella Gaudio and Dr. Richard Wigmans[1]

on behalf of the RD52 (DREAM) Collaboration

(Cagliari - Cosenza - Iowa State - Lisbon - Pavia - Pisa - Roma I - Texas Tech)

9 April 2013

[1]Contact person. Tel. [806] 742 3779, FAX [806] 742 1182, E-mail: wigmans@ttu.edu

1 Introduction

On August 31, 2011, the CERN Research Board decided to accept the DREAM Collaboration's detector R&D proposal [1] and included it as project RD52 in its official scientific program. This document constitutes the second RD52 progress report. In this report, we describe our activities since the last time we reported to the SPS Committee (April 3, 2012 [2]), as well as our future plans.

Most of our activities in 2012 were geared toward the construction of the new dual-readout fiber calorimeter, in order to assemble and test as large an instrument as possible before the shutdown of the SPS operations at the end of the year. The tests of this instrument took place in the H8 beam in the period November 23 - December 3. An earlier testbeam period, in July 2012, was primarily dedicated to optimizing the different particle beams (e, π, μ of different energies) and eliminating sources of electronic noise that had affected our measurements at previous occasions.

The RD52 results have been presented at all major instrumentation conferences in the past year: Elba (May 2012), CALOR (Santa Fe, June 2012), IEEE (Anaheim, October 2012), Vienna Instrumentation Conference (February 2013). Presentations can be found in the proceedings of these conferences and at the RD52 website:
http://highenergy.phys.ttu.edu/dream/results/talks/talks.html

Details about our various past, current and planned activities are given in the next sections.

2 Test beam optimization

In any calorimeter R&D project, good quality beams, covering as large an energy range as possible, are of great importance.

Electrons are essential for calibrating the individual calorimeter cells, and for checking the linearity of the calorimeter readout. Moreover, electrons are the most sensitive tools to check the response uniformity. In our setup, muons are important for calibrating the leakage counters that surround the calorimeter. And since our goals concern primarily the hadronic performance of the calorimeter, pion beams are the tools of choice to test this performance. This also means that we strongly prefer beams of negative polarity, since the positive beams contain a sizable, energy dependent fraction of protons. Since proton showers differ in essential ways from pion showers (*e.g.* interaction length, electromagnetic shower fraction characteristics,...), negative polarity beams are needed for hadronic energy scans. In the SPS environment, this may lead (and has led) to a conflict of interest with the H6 users, especially also because the beam momentum chosen for H8 limits the momentum range available in H6. We strongly request that the SPS coordinator keeps this in mind when scheduling future H8 activities involving RD52.

Setting up good quality beams is notoriously difficult in our experimental area (H8C), because of the long distance from the secondary beam production target (T4), and the shortage/absence of beam elements in the last section of the beam line. The purity and quality of the electron beams also suffer from the fact that they are produced by less selective mechanisms than in the beam lines that derive from production target T2. For example, high-energy elec-

trons are selected on the basis that they lose more energy through synchrotron radiation than pions of the same momentum, as opposed to the T2 beam lines where all charged secondaries are bent away and the neutrals (*i.e.* photons from π^0 decay) are producing electrons/positrons in a downstream radiator.

Another complicating factor is the fact that experiments downstream from our setup (TOTEM, CALICE) also use the H8 beam line. Our equipment has to be moved out of the way to make this possible. For these reasons, we have built a system of trigger counters and beam defining elements that can be moved in and out of the beam line in a reproducible fashion. This system consists of two small trigger counters, a veto counter consisting of a scintillator paddle with a circular hole, two wire chambers, a fiber hodoscope and a preshower detector (PSD). All these elements are mounted on a rail that can be moved sideways to give passage to the beam. The calorimeters themselves are placed on a table that can be lowered.

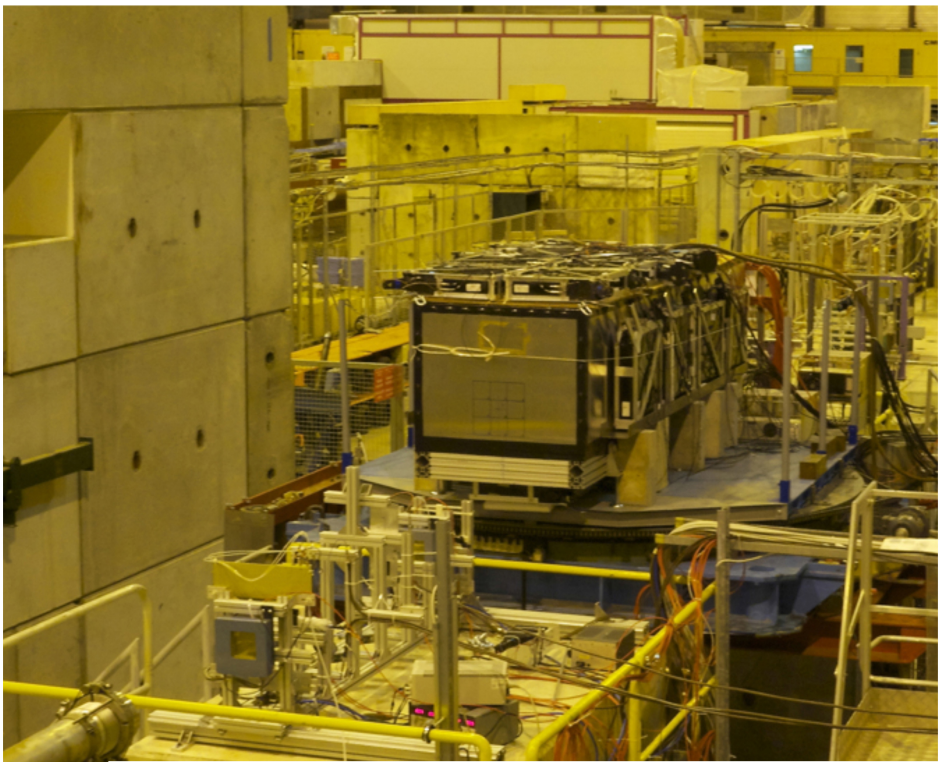

Figure 1: The new SuperDREAM fiber calorimeter, installed in the H8C beam area. The system of trigger counters and beam defining elements is visible in the left bottom part of the figure.

Another crucial component of our particle identification system is a muon counter, a 50×50 cm^2 scintillator paddle located in a fixed position more than 20 m downstream, behind more than 10 nuclear interaction lengths of absorber material.

As described in our previous status report, our particle identification systems based on auxiliary detectors turned out to be crucially important for obtaining good quality beams of sufficient purity.

3 The SuperDREAM fiber calorimeter

After extensive tests of many details, the RD52 Collaboration decided to embark on the construction of a new full-scale fiber calorimeter, which should significantly improve the performance of the original 1-ton DREAM module. This detector was designed to be large enough to contain high-energy hadron showers at a sufficient level to eliminate the effects of leakage fluctuations, which dominated the energy resolution of the original DREAM module. After fluctuations in em shower content are eliminated with the dual-readout method, the hadronic energy resolution of this fiber calorimeter is then dominated by sampling fluctuations and fluctuations in Čerenkov light yield. We aim to reduce both sources of (Poisson) fluctuations to about $10\%/\sqrt{E}$, by making modifications to the original DREAM fiber module in terms of the fiber packing fraction and sampling frequency, the numerical aperture of the fibers and the quantum efficiency of the PMTs. Another important difference with the original DREAM fiber calorimeter concerns the readout, which should allow us to obtain the time structure of all calorimeter signals. Details of the proposed detector development program are described in [1].

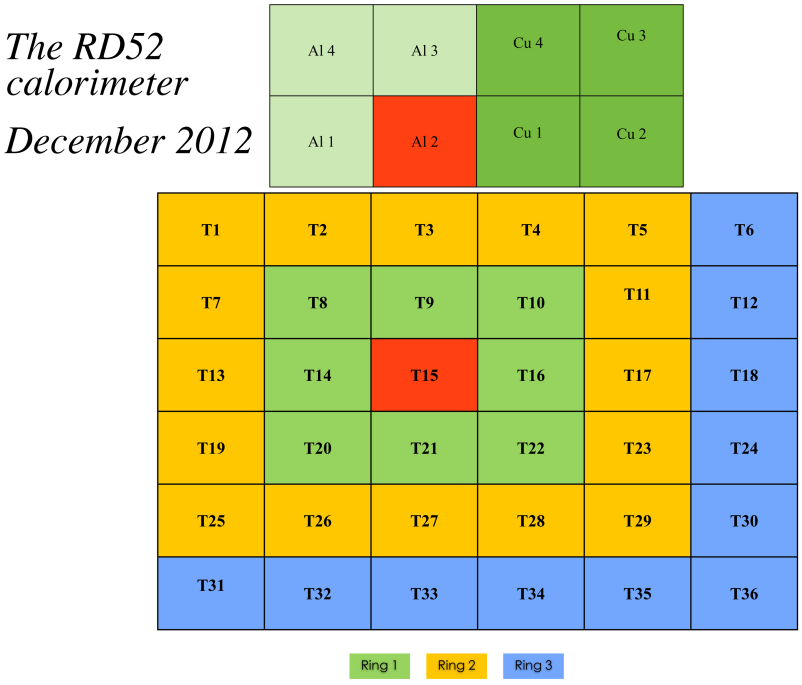

Figure 2: The RD52 calorimeter as tested at the end of 2012. It consisted of 9 lead-based modules, each consisting of 4 towers (towers 1-36), and two copper-based modules, placed on top of the lead array.

The fiber calorimeter is modular, and is being constructed in Pavia and Pisa. Each module contains 4 towers, and is read out by 8 PMTs, 4 for the Čerenkov channels and 4 for the scintillation channels. Each module is 2.5 m long (10 $\lambda_{\rm int}$), has a cross section of 9.2×9.2 cm^2 and a fiducial mass of about 150 kg. Each module consists of four towers ($4.6\times4.6\times250$ cm^3), and each tower contains 1024 plastic optical fibers (diameter 1.0 mm, equal numbers of scintillating and clear fibers). Each tower produces two signals, a scintillation signal and a Čerenkov signal, which are detected by separate PMTs.

The first modules were constructed with lead as absorber material. In the course of 2012, our collaborators in Pisa also managed to construct modules with copper as absorber material (fiducial mass ∼120 kg) One of these modules was equipped with Čerenkov fibers of which the upstream end was aluminized (by Eileen Hahn at Fermilab). By the end of 2012, the Pavia group had finalized the construction of 9 lead-based modules.

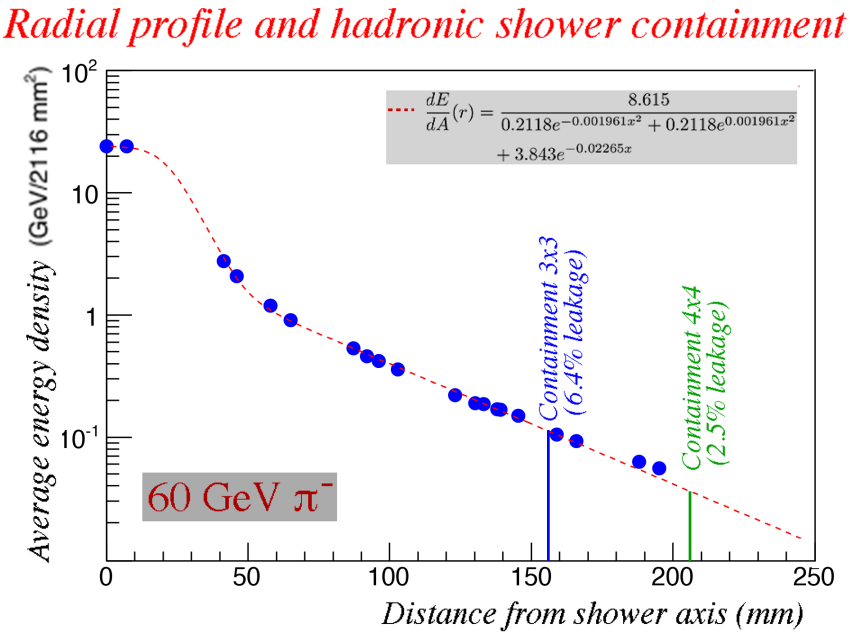

Figure 3: The radial profile of 60 GeV π^- showers developing in the RD52 calorimeter as tested at the end of 2012. This profile shows the average signal as a function of the distance to the shower axis. The average shower leakage is derived from the fit to this profile and indicated for the tested calorimeter (6.4%) and for a calorimeter that would consist of a 4×4 module array (2.5%).

These modules were assembled together, as shown in Figure 2, and tested as such in November/December 2012. Measurements of the radial shower profile (Figure 3) showed that the showers initiated by 60 GeV π^- were, on average, contained at the level of 93.6% in this structure. For comparison, we mention that the average shower leakage in the original DREAM calorimeter, was about 10% for 80 GeV pions. In order to detect this shower leakage, the calorimeter was surrounded by large slabs of plastic scintillator, found in CERN surplus stocks and cut to size ($50\times50\times10$ cm^2, mass 25 kg). Twenty such counters were used in these tests. They can be seen in Figure 1 on top and on the right hand side of the box containing the calorimeter.

The calibration of these leakage counters was non-trivial. During the beam tests, we sent a beam of high-energy muons through each row of 4 leakage counters (one row left and right of the calorimeter module, two rows above and underneath). In this way, the muons deposited, on average, 100 MeV in each of the counters (see Figure 4a). However, using the calibration constants derived from this procedure, the actual leakage signals were much smaller than expected. This is because in reality, the leakage is dominated by large numbers of neutrons escaping the calorimeter, and the signals from recoil protons produced in these scintillation counters are strongly

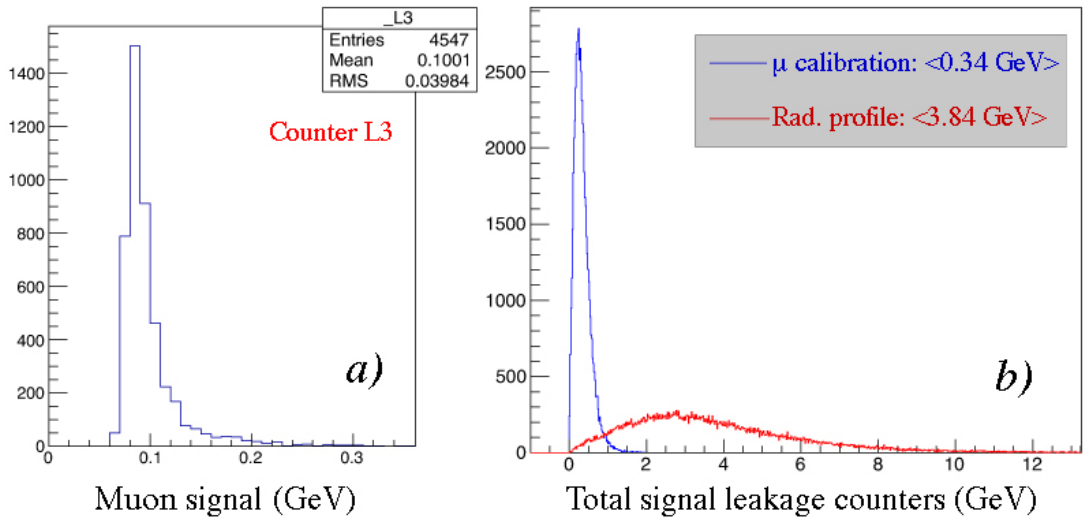

Figure 4: The signal distribution of muons traversing one of the leakage counters installed around the RD52 calorimeter (a). The total signal distribution in the leakage counters observed for 60 GeV π^- showering in the RD52 calorimeter (b). The calibration of the leakage signals was performed in two different ways. See text for details.

suppressed because of Birks' law [3]. For this reason, we used the average leakage energy fraction (6.4% for 60 GeV pions) as the basis for calibrating the leakage counters. The difference between these two calibration schemes is shown in Figure 4b. In the future, we plan to read the signals from the leakage counters with DRS modules, which will give us the time structure and thus allow us to distinguish event by event between the contribution of mips and neutrons to the leakage signals.

The calibration of the signals from the calorimeter towers was performed with a beam of 20 GeV electrons, which was steered into the center of each of the 44 towers. On average, each tower hit by these particles in its center contributed 85% of the total signal, and this *electromagnetic calibration* formed the basis for the conversion (GeV per ADC count) of the calorimeter signals into deposited energy.

4 Experimental results

4.1 Electromagnetic performance

A major difference with the original DREAM fiber module concerns the fact that each fiber is now individually embedded in the absorber structure, whereas the fibers were bunched together in groups of seven in the DREAM module. This is illustrated in Figure 5, which also shows, for comparison and on the same scale, the structure of the (compensating) SPACAL calorimeter. The fiber density has also been increased by about a factor of two with respect to the original

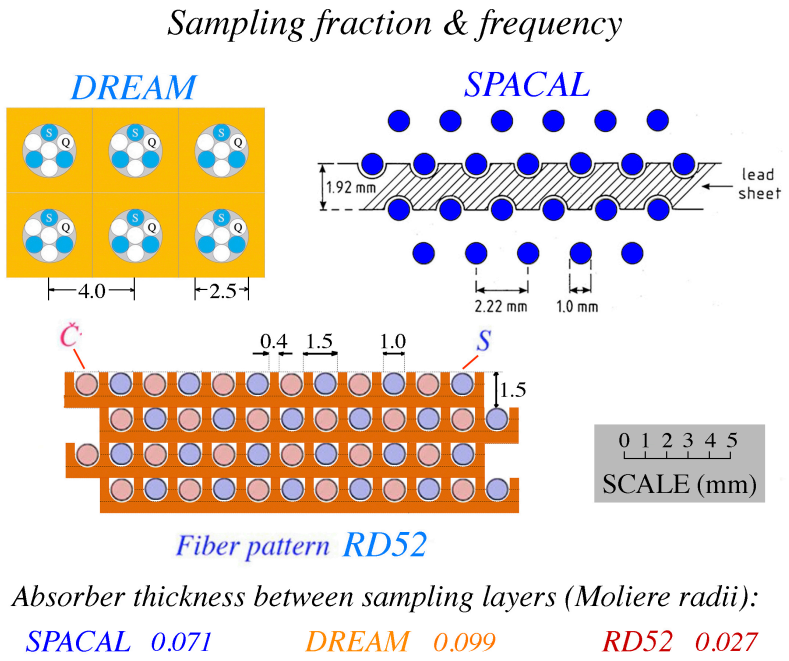

Figure 5: The structure of the new RD52 calorimeter, compared to that of two other fiber calorimeters: DREAM [4] and SPACAL [5].

DREAM module. As a result, the contribution of sampling fluctuations to the energy resolution[1] has been reduced by a factor 2.2.

One additional advantage of the new fiber pattern is the fact that the scintillation and Čerenkov readout represent completely independent sampling structures. Therefore, by combining the signals from the two types of fibers, a significant improvement in the energy resolution is obtained. This was not the case for DREAM, where the two types of fibers essentially sampled the showers in the same way.

The changes in the structure of the fiber module did indeed pay off in the form of a substantially improved em energy resolution. This is illustrated in Figure 6, where the response functions of the RD52 Cu-based calorimeter for electrons of different energies are shown together with the response functions for 40 GeV electrons in the original DREAM module [4].

Another advantage derives from the greatly reduced distance between neighboring fibers. This makes the response (and thus the energy resolution) much less sensitive, if at all, to the impact point of the electrons. Because of the extremely collimated core of the em showers, there is a systematic response difference between particles entering the detector in the absorber material or in the fibers in this type of calorimeter. This difference is responsible for the non-Gaussian line shape of the scintillation signals in the DREAM calorimeter (Fig. 6d), an effect that gets rapidly worse when the angle of incidence of the particles approaches 0°. Interestingly, this effect is absent for the Čerenkov signals. This is because the very collimated, narrow core

[1] This contribution scales like $\sqrt{d/f_{\rm samp}}$, where d represents the fiber thickness and $f_{\rm samp}$ the sampling fraction [3].

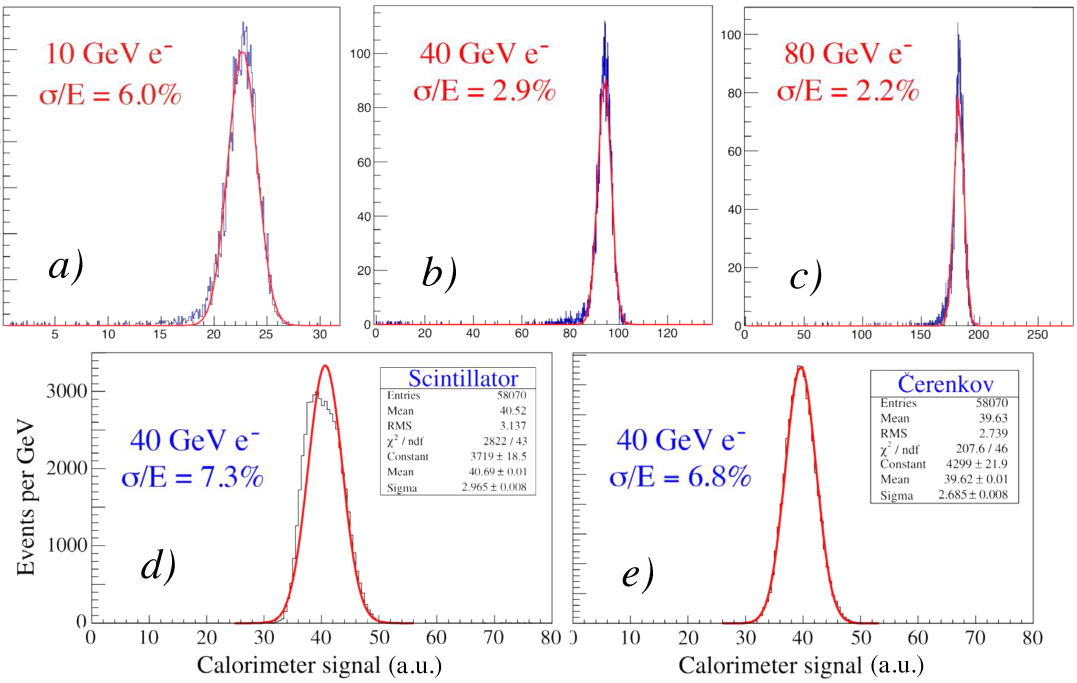

Figure 6: Response functions of the RD52 Cu-fiber calorimeter to electrons of 10 (a), 40 (b) and 80 (c) GeV, compared with the response functions of the DREAM calorimeter to 40 GeV electrons, in the scintillator (d) and Čerenkov (e) channels. In $a-c$, the scintillator and Čerenkov signals were combined (see text).

that characterizes the early phase of em showers does *not* contribute to the Čerenkov signals, since the Čerenkov light generated in this phase falls outside the numerical aperture of the fibers [4]. Because of the very small distance between neighboring sampling layers (fibers), this impact

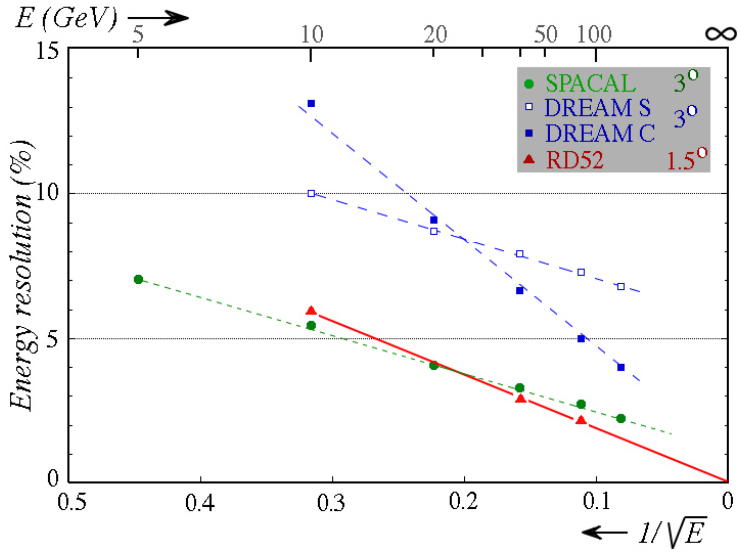

Figure 7: Comparison of the em energy resolution measured with the RD52 fiber calorimeter, the original DREAM calorimeter [4], and the SPACAL fiber calorimeter [5].

point dependence is almost completely absent for the RD52 calorimeter. As a result, the energy resolution scales perfectly with $E^{-1/2}$ (Figure 7). In more crudely sampling fiber calorimeters such as DREAM [4] and SPACAL [5], the energy resolution clearly exhibits a deviation from $E^{-1/2}$ scaling as a result of the mentioned effect[2]. At energies above 20 GeV, the em energy resolution is clearly better than that of any of the other mentioned fiber calorimeters. Further improvements may be expected when the effects of a preshower detector placed upstream of the calorimeter are taken into account.

4.2 The time information

To measure the light attenuation in the two types of fibers, a new method has been tried out for determining the depth at which the light was produced in the fiber calorimeter. A crucial aspect of this type of calorimeter is its *longitudinally unsegmented* structure. However, the detailed time structure of each event makes it possible to obtain crucial information about the depth at which the light is produced. By using the fact that light travels at a speed of c/n in the fibers, while the particles producing the light travel at c, the starting time of the signals makes it possible to measure the depth at which the light is produced, as illustrated in Figure 8. We measured a

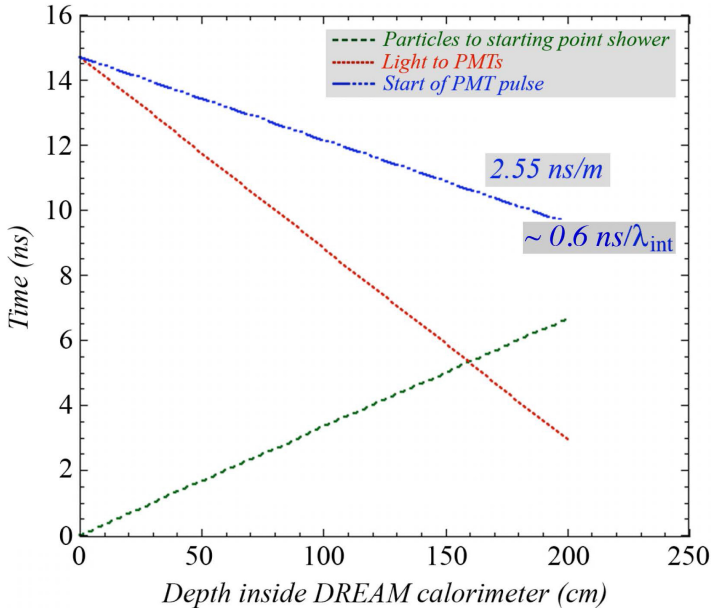

Figure 8: The dependence of the starting time of the PMT signals on the depth (z) inside the calorimeter at which the light is produced. Also shown are the time traveled by the beam particles from the front face of the calorimeter to this depth z and the dependence of the time traveled by the light through the fibers from z to the PMT.

significant difference between the distribution of the starting time of pion and electron induced showers. Since the depth distribution pattern of the light produced by the latter is very similar for all showers, the σ of the starting time distribution of the electron showers is a good measure

[2]It should also be noted that the RD52 data were taken at an angle of 1.5° between the beam line and the fibers, whereas this angle was 3° for the other detectors. The mentioned effect is extremely sensitive to this angle [5].

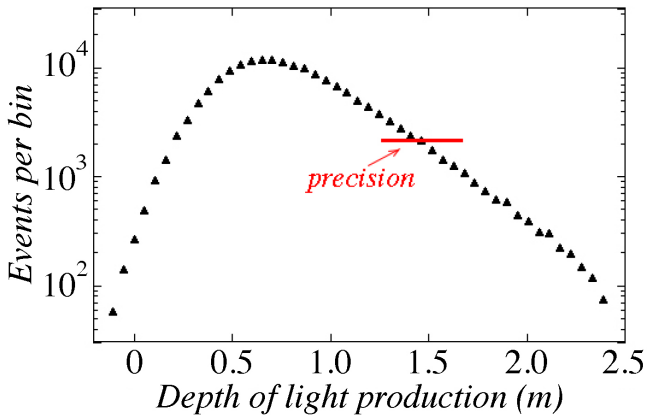

Figure 9: Distribution of the numbers of events for which the (Čerenkov) light is produced at a certain depth inside the calorimeter by the beam particles (60 GeV π^-).

for the precision in the depth of the light production that can be obtained for individual showers. Figure 9 shows the measured depth distribution of the light produced in 60 GeV π^- showers, as well as the precision with which this depth could be measured for individual events, ~ 20 cm.

This timing information also makes it possible to measure, and correct for, the attenuation characteristics of the fibers. Figure 10a shows a scatter plot of the calorimeter's hadronic Čerenkov signal as a function of the depth at which this light was produced. This plot shows a very slight increase with depth, a result of light attenuation in the fibers. By taking the averages for all events in given depth bins, the attenuation length of the fibers can be measured, 8.9 m in this case (Figure 10b). A precision of 20 cm on the depth measurement for individual events will thus lead to an irreducible error of 20/890, or a little more than 2%, on the measured signal. Aluminization of the upstream ends of the fibers is a possible way to eliminate this effect.

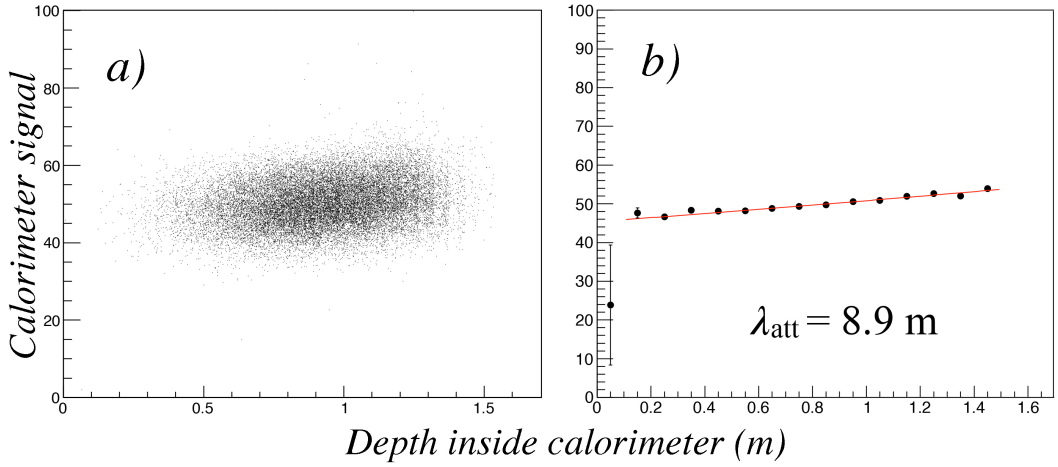

Figure 10: Scatter plot of the Čerenkov signal *vs.* the depth at which this light is produced inside the calorimeter by the 60 GeV π^- beam particles (a), and the average signal as a function of this depth.

Apart from allowing corrections for light attenuation in the fibers, the measurement of the

depth of the light production in this longitudinally unsegmented calorimeter may also turn out to be useful for other purposes, in particular

1. Particle identification. Electrons may be recognized since they always produce light concentrated in the first 20 cm of the calorimeter module. In addition, the time structure of the signals is always the same, and significantly different from that of hadronic signals. The characteristic lateral shower profile offers a handle as well. A separate paper on this topic is in preparation.

2. The depth measurement in several towers contributing to the shower signal may provide an indication of the direction at which the particle(s) entered the calorimeter, thus allowing measurement of the entire four-vector.

As shown elsewhere [6], the time structure, measured with a Domino Ring Sampler operating at 5 GHz [7], is also an important tool for measuring the neutron contribution to the scintillation signals, both from the calorimeter itself and from the leakage counters (see Section 3).

4.3 Hadronic performance

Analysis of the hadronic performance is still in an early stage. Effects caused by light attenuation in the fibers and lateral shower leakage have yet to be taken into account.

Yet, initial results are very encouraging, as illustrated by Figure 11. It has been shown [8, 9] that the energy E of a hadron in a dual-readout calorimeter can be found in the following way:

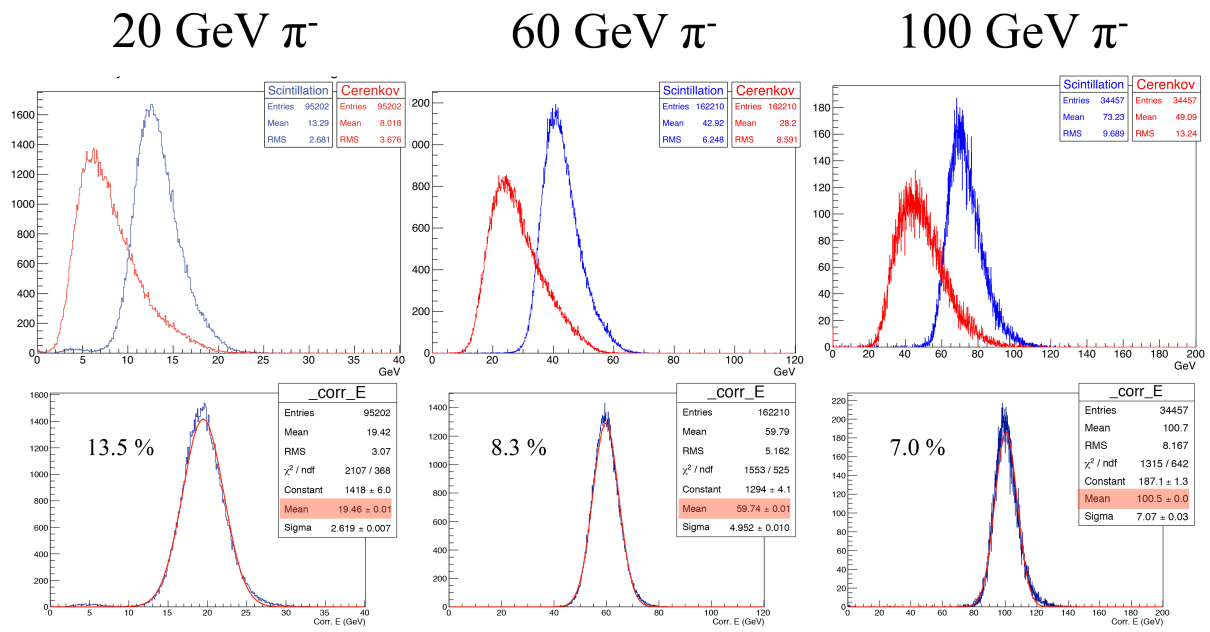

Figure 11: Signal distributions for π^- beam particles of 20, 60 and 100 GeV entering the calorimeter in the center of tower 15. The top row shows the signal distributions measured for the scintillation (blue) and Čerenkov (red) signals. The bottom row shows the signal distributions that were obtained after combining the S and C distributions according to eq. 1, with $\chi = 0.45$.

$$E = \frac{S - \chi C}{1 - \chi} \quad \text{with} \quad \chi = \frac{1 - (h/e)_S}{1 - (h/e)_C} \tag{1}$$

where S and C represent the scintillation and Čerenkov signals measured for each individual event, and χ is a fixed parameter that is characteristic for the calorimeter, determined by the e/h values of the scintillating and Čerenkov calorimeter structures. The signal distributions in Figure 11 are well described by Gaussian functions, and the average values are close to the beam energies. The latter aspect is illustrated in Figure 12a, which shows that the dual-readout signals are linear and give the same average values as electrons of the same energies, unlike the individual scintillation and Čerenkov signals, for which the response characteristics are shown as well in Figure 12a.

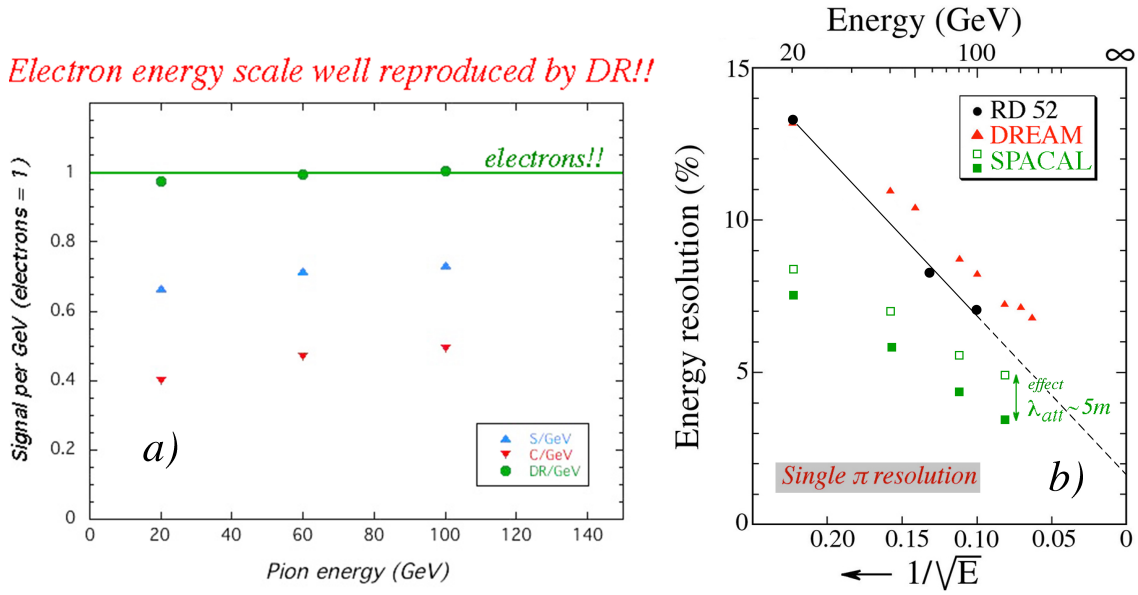

Figure 12: The hadronic response (signal per GeV) for the S and C signals in the RD52 calorimeter, as well as the dual-readout response for $\chi = 0.45$ (a). Comparison of the preliminary energy resolution obtained for single pions with the partially completed RD52 fiber calorimeter, and the published resolutions for single pions obtained with the DREAM calorimeter [10] and with the SPACAL fiber calorimeter [5]. The latter results are shown before and after correcting for light attenuation effects in the scintillating fibers.

Figure 12b shows that the energy resolutions in this 1.5-ton calorimeter are better than for single pions measured in the (1.0-ton) DREAM calorimeter. They are not yet at the level of the compensating 20-tonnes SPACAL calorimeter, which holds the world record in this domain [5]. Based on the results obtained with the latter instrument, a further improvement of the RD52 resolutions may be expected from taking into account the effects of light attenuation in the fibers. However, the effects of shower leakage still dominate the hadronic energy resolution. Yet, extrapolating the results to high energies, it seems that any deviation from $E^{-1/2}$ scaling in the resolution is very small. We consider these (preliminary) results very encouraging.

5 Future plans

The results obtained in the last months of 2012 are very encouraging. The calorimeter we constructed and assembled performs according to our expectations. The numerous experimental problems we encountered as a result of moving our operations from H4 to H8 are finally under control, and we have created in H8C an environment where further progress in the development of this exciting new technology may be envisaged. The long shutdown of the SPS presents an opportunity to reflect on our future plans.

The detector we recently tested represents about one third of the fiducial mass of the instrument we originally proposed. The measured radial shower profile (Figure 3) shows that increasing the detector from a 3x3 module matrix (36 towers) to 4x4 (64 towers) would reduce the average shower leakage from 6.4% to 2.5%. Combined with a further completion of the leakage shield and (especially) measuring the time structure of the leakage signals (see Figure 4b), this would probably lead to a substantial further improvement of the hadronic energy resolutions. Since we already have 11 calorimeter modules, this would require building 5 more.

Until now, the construction of the calorimeter modules has taken place in Italy, by our Pavia and Pisa collaborators. Under normal circumstances, constructing 5 more modules would not have been an insurmountable burden for these groups. Unfortunately, as a result of the budgetary problems in Italy, INFN has decided not to support RD52 any longer. This means that we will have to find alternative ways to continue the construction of the fiber calorimeter. We are currently investigating the options in this respect.

Also the US Department of Energy has revised its allocations of grant money to this project downward, as a result of the general reduction of discretionary government spending in the USA. Nevertheless, we count on receiving at least another $500K from DOE in the next two years.

Of course, the situation could completely change if the ILC became a reality. In our opinion, this calorimeter should be a very attractive candidate for an experiment at such a collider. For that reason, we aim to perform some tests that are of interest to the ILC community the next time we get an opportunity to test our instruments in the H8 beam:

- Measurements of multi-hadron "jets" at 80 and 90 GeV, which should provide an answer to the question how well hadronically decaying W and Z bosons could be distinguished in this device. Since the calorimeter will not be more massive than 2.5 tonnes, some extrapolation of experimental data measured for different degrees of shower containment may be necessary for this.

- A measurement of the electromagnetic response function as a function of the angle of incidence, in the $0 < \theta < 10^{\circ}$ range. This will be useful to see if and to what extent this response function would be affected by "channeling effects" (as depicted in fig. 6d).

- Measurements of the time structure of the signals in neighboring towers for particles entering the detector at an angle θ with the fibers, and determine with what precision the value of this angle could be measured in this longitudinally unsegmented calorimeter.

5.1 Plans for the longer-term future

Plans for 2014 and beyond include the following:

- Development of absorber structures with considerably higher density. This would make it possible to construct more compact calorimeters of this type. Even though the cost of these new structures is likely to be much higher, this may lead to important overall savings. For example, a 10 m long barrel calorimeter with an inner radius of 1 m would encompass an instrumented volume of about 350 m^3. This could be reduced to 180 m^3 if tungsten were used as absorber material instead of copper.

- Studies of projective calorimeter structures based on the DREAM concept. If a calorimeter of the SuperDREAM type was chosen for a 4π experiment, a projective geometry would be required. This poses a number of complications, which are however not unsolvable. In the context of the RD1 and RD25 projects, fully projective fiber calorimeters have been built [11, 12]. We plan to build on the expertise developed in that context.

- Development of an alternative readout system. Splitting the thousands of fibers sticking out of the back, separating them into scintillating and Čerenkov ones and bunching them accordingly is very cumbersome. Moreover, this system takes up valuable space (≈ 50 cm in the detectors we have built so far), and the fiber bunches may sometimes act as antennas, picking up signals that have nothing to do with the ones for which they are intended. For this reason, we have started to look into a readout system based on silicon photomultipliers. The fibers would no longer stick out of the back, but each fiber would be connected to its own individual SiPM, located at the end face of the absorber structure. Given the large surface area that would have to be covered, such a system is at present still prohibitively expensive. However, given the rapid development of this technology, this might change in the years to come. We are in any case planning to test this idea on a modest scale.

References

[1] DREAM Collaboration (Wigmans R) 2010, CERN-SPSC-2010-012/SPSC-M-771.

[2] DREAM Collaboration (Wigmans R) 2012, CERN-SPSC-2012-014; SPSC-SR-100.

[3] Wigmans R 2000, *Calorimetry, Energy Measurement in Particle Physics*, International Series of Monographs on Physics, Vol. 107, Oxford University Press.

[4] Akchurin N *et al.* 2005, Nucl. Instr. and Meth. in Phys. Res. **A536**, 29.

[5] Acosta D *et al.* 1991, Nucl. Instr. and Meth. in Phys. Res. **A308**, 481.

[6] Akchurin N *et al.* 2009, Nucl. Instr. and Meth. in Phys. Res. **A598**, 422.

[7] Ritt S *et al.* 2010, Nucl. Instr. and Meth. in Phys. Res. **A623**, 486.

[8] Groom DE, Nucl. Instr. and Meth. in Phys. Res. **A572** (2007) 633; **A697** (2013) 84; **A705** (2013) 24.

[9] Wigmans R 2008, New Journal of Physics **10**, 025003.

[10] Akchurin N *et al.* 2005, Nucl. Instr. and Meth. in Phys. Res. **A537**, 537.

[11] Badier J *et al.* 1994, Nucl. Instr. and Meth. in Phys. Res. **A337**, 326.

[12] Anzivino G *et al.* 1995, Nucl. Instr. and Meth. in Phys. Res. **A357**, 350.